energies

MDPI

Article

Robust MILP Optimization of Renewable Power Plants: The Role of BESS Sizing in Uncertainty Mitigation

Tommaso Dieci *, Corrado Maria Caminiti, Matteo Spiller and Marco Merlo *

Department of Energy, Politecnico di Milano, 20156 Milan, Italy; corradomaria.caminiti@polimi.it (C.M.C.); matteo.spiller@polimi.it (M.S.)

* Correspondence: tommaso.dieci@polimi.it (T.D.); marco.merlo@polimi.it (M.M.)

Abstract

The reduction of carbon dioxide related to the energy sector is one of the greatest challenges of this century. To ensure a proper transition towards a sustainable electric power system, innovative solutions are fundamental for the efficient integration of renewable energy sources. Hybrid Renewable Energy Systems (HRES) play a crucial role in this scenario; they can ensure a stable and reliable electricity supply thanks to the combination of different renewable technologies, particularly thanks to the integration of storage systems. However, the optimal sizing process of such systems is a complex challenge due to the multiple uncertainties that can be present, involving demand fluctuations and electricity zonal price variations. The aim of this work was to develop a Mixed-Integer Linear Programming (MILP) optimization approach for the robust sizing of a HRES under multiple sources of uncertainty. The developed hybrid model consists of a wind farm, a photovoltaic (PV) plant, a Battery Energy Storage System (BESS), and an industrial load with the entire infrastructure for connection to the national power grid. Additionally, the model includes the capability to manage the over-generation of renewable resources through curtailment mechanisms. The objective of the sizing tool is to minimize the Net Present Cost (NPC) of the plant, while ensuring the reliability of the system. The developed tool can represent a useful assistant for the evaluation of different possible configurations, helping the decision-making process during the design of a HRES. The results will show the best trade-off between economic and reliability aspects, highlighting the impact that the uncertainty has on the optimal size of the plant. In particular, the best configuration analyzed is able to reduce the NPC of more than 50% compared to a plant with a single renewable source.

Keywords: robust optimization; Hybrid Renewable Energy System; Mixed-Integer Linear Programming; battery energy storage systems; duration sensitivity

Academic Editor: JongHoon Kim

Received: 27 April 2026
Revised: 14 May 2026
Accepted: 18 May 2026
Published: 21 May 2026

1. Introduction

Global emissions of carbon dioxide from the energy sector reached a record value in 2024, equal to 38 gigatonnes [1], of which 14.6 gigatonnes originated from the electric sector, with an increase of 1.6% compared to 2023 [2]. In the same year, renewable energy sources accounted for 31.9% of global electricity production, with an increase of 10% [3], and meeting 73% of the electricity demand growth [2]. According to [4], the global renewable production is expected to increase by 84% over the next five years, and to double again by 2050. Under this scenario, by mid-century, renewable energy sources are projected to supply 67% of global electricity demand.

Addressing the integration of Renewable Energy Sources (RES) requires an understanding of their general behavior and their interaction with the electricity grid. The main problem associated with wind and solar power is that they are non-depletable, unpredictable, and site-dependent resources [5]. In addition, the variation of solar and wind energy does not match the demand [6]. For this reason, renewable energy sources are combined to form Hybrid Renewable Energy Systems (HRES) to reach higher reliability, to take advantage of sources with complementary behavior, and to increase the overall efficiency of the system [7]. As presented in [8], HRES are composed of more renewable resources, with or without conventional sources, such as Diesel generator, which works as back-up devices. Several configurations can be found: solar photovoltaic (PV)-wind-diesel, hydro-wind-PV, wind-PV, wind-PV-Battery Energy Storage System (BESS), PV-wind-fuel cell [9]. The configuration involving wind-PV-BESS is one of the most common configurations of HRES found in the literature. Such a configuration is capable of ensuring a good satisfaction of the demand using only renewable energy, without any backup systems such as Diesel generators, or more expensive storage technology, such as hydrogen [10]. Typically, an HRES with an imposed energy load has its assets sized in order to exploit the renewable resources, from both an economic and an efficiency point of view [11]. The sizing of an HRES is an optimization problem that is influenced by the uncertainty of the input data, such as generation availability, load requirements, and energy prices [12]. It was shown that improving the forecast of meteorological conditions, thus reducing uncertainty, will lead to important savings of annual operating costs [13]. While considering the sizing, it was shown that considering the uncertainty can lead to a variation of 6% of the total capacity of a wind park plant [14]. As shown, the uncertainty of the renewable resources affects the sizing of the capacity of an HRES: underestimating the uncertainty can lead to undersized plants, which are not able to satisfy the demand; vice versa, overestimating the uncertainty can lead to a too conservative solution, with higher costs and problems related to the balance of the electric grid.

The problem of optimal sizing for an HRES in the presence of uncertainty can be approached in several ways. The simplest is when the uncertainties are not considered, it is referred to as deterministic optimization, in this case, the input data are assumed to be fixed. The literature is full of different works: in [15] the area of PV and the number of wind turbines (WT) are sized by maximizing the Net Present Value (NPV); in [16] minimizes the total installation cost of the capacity of PV, WT, and BESS, while using the Loss Of Load Probability (LOLP) to ensure the reliability of the system; Akram et al. [17] optimizes a HRES composed of PV-WT-BESS by maximizing the ratio between reliability, computed as the Energy Served (ES), and costs; in [18] the design variables are the number of PV and WT and the amount of energy bought from the public grid optimize with the minimization of the total costs; [19] finds the optimal combination of PV, WT, BESS, Diesel generators, and electrolyzer/fuel cell, using a multi-objective optimization by minimizing the Net Present Cost (NPC), the carbon dioxide emissions, and the demand not satisfied. The main drawbacks of deterministic optimization are that the variability of the input data, or the different sources of uncertainty, is not considered, leading to solutions that lack robustness and reliability. In the available literature, there are different methods used to deal with uncertainty.

A great variety of studies treat the sizing optimization of a HRES as a Mixed-Integer Linear Programming (MILP) problem, due to its ability to guarantee the global optimal solutions [20]. In a MILP, all the equations must be written in a linear form, but modeling the uncertainty can lead to nonlinearities, which are no longer compatible with a MILP framework and require approximations to be solved. For this reason, this work focuses

on uncertainty modeling approaches that can preserve linearity and, therefore, can be integrated within a MILP formulation.

A first possible approach to increase the robustness of the solution is to analyze the so-called worst-case scenario. When dealing with this approach, the idea is to consider the worst possible values for all the input data, but this leads to an overly conservative solution. Indeed, this is a deterministic optimization simply done with the worst possible input data. In [21], four future scenarios were defined using a 2 × 2 matrix by taking different levels (high or low) of the two primary sources of uncertainty; the aim was to derive specific strategies for even the most unfavorable conditions. A more advanced approach could be based on stochastic programming. In such a case, the input data are no longer described by fixed values, but instead are described using statistical instruments such as probability distributions, to evidence the variability of this data [22]. In particular, the uncertainty is described by multiple scenarios, and the relative probability should reflect the future operations of the system [23]. Akbar et al. [24] and Fanzeres et al. [25] use a stochastic method based on Monte Carlo simulation to generate several distributions of the input data, multiple possible scenarios are statistically determined, and each one is simulated to estimate the final solution. Bornapour et al. [26] modeled, through a stochastic approach, the uncertainty of wind speed, solar irradiance, and energy price to optimize the optimal scheduling of the elements of the system. These methods face significant drawbacks: the problem size increases exponentially with the number of time periods and number of scenarios, leading to models that are computationally expensive and, eventually, intractable [27].

Finally, an advanced approach to managing uncertainty is robust optimization. In this case, the uncertainty is modeled using uncertainty set, which is a mathematical space that contains all the possible values that the uncertain data can assume [28]. From these sets, the robust mathematical formulation is able to obtain a worst-case scenario, which is not deterministic, but is formulated considering the operating conditions of the system. The robustness of the solution is controlled by a specific parameter called uncertainty budget, which is used to limit the overall deviation of the data from their nominal value. It can vary between 0, which is a solution obtained without considering uncertainty, consequently resulting in more vulnerability in case of forecast errors, and 100%, which is equivalent to the worst-case scenario and, therefore, a too conservative solution [29]. The solution that can be found will be feasible for all the values inside these sets, ensuring a safer operating condition of the system. Robust optimization can be applied to different sectors: Saeedi et al. [30] used a robust approach to manage the uncertainty of the cooling demand of buildings; Mojtaba et al. [31] and Shabanzadeh et al. [32] modeled the uncertainty of the energy price; Billionnet et al. [33] used a two-stage robust approach to determine the optimal sizing of a HRES composed of wind turbines, photovoltaic panels and a BESS; also Keyvandarian et al. [34] sized a HRES using robust optimization taking into account reliability index. Considering the literature analyzed, robust optimization represents a viable approach for modeling the input data uncertainty in a HRES sizing optimization problem. In particular, it requires lower computational effort than stochastic methods, making it well-suited for the problem considered.

Although several studies have applied this mathematical approach, none have considered both load and price as uncertain variables in order to assess their impact on the performance of the system. Moreover, while a wide range of components have been investigated, the role of BESS in mitigating uncertainty has not been explicitly analyzed in previous works. In addition, when dealing with the BESS size, the value of EPR is not considered as a relevant parameter, but is mainly assumed as fixed. Starting from these considerations, this study addresses the following research questions:

- How the uncertainty of load and price can be modeled and measured in an HRES?
- How does it impact the economics of an industrial case study?
- Knowing that a BESS is capable of increasing the economics of a plant [35], how does it affect the uncertainty of other input data?
- How should BESS be sized under uncertainty?

For this reason, an optimization tool was developed to support the optimal sizing process of a renewable power plant connected to an industrial load.

This work is structured as follows: Section 2 describes the mathematical formulation of the optimization problem, detailing the various equations that compose it; Section 3 presents the case study with all the input data considered and the sources used for the data gathering; Section 4 presents the results obtained from the numerical simulations performed; Section 5 gives the main conclusions based on the study's outcomes.

2. Methodology

Considering the definition of HRES given in Section 1 and the configurations most frequently reported in the literature, the combination WT-PV-BESS was used for the system under analysis. The wind and solar resources are combined to produce a certain amount of power for each hour (p_t^{hyb}), as reported in Equation (1).

$$p_t^{hyb} = P_t^{wt} \cdot x^{wt} + P_t^{pv} \cdot x^{pv} \quad (1)$$

P_t^{wt}, P_t^{pv} represent the normalized power production profiles of the renewable resources, while x^{wt}, x^{pv} are the installed capacities of WT and PV expressed in MW, which are the design variables of the optimization problem.

The BESS can be charged ($p_t^{bess,in}$), or discharged ($p_t^{bess,out}$). Its capacity, x^{bess}, is the last design variable of the problem, and it is also limited between zero and N_{max}^{bess}.

The plant is connected to an industrial load, with the objective of meeting its energy demand (p_t^{load}). Finally, the HRES is connected to the grid, allowing energy exchange. In particular, the plant can purchase the energy required ($p_t^{grid,buy}$) if a lack occurs at a fixed cost ($C^{en,grid}$), or sell ($p_t^{grid,sell}$) the energy excess at a variable price, which will be referred to in the following parts as zonal price (PZ). In addition, there is the possibility to curtail the over-generation ($p_t^{curtail}$). The system described is represented in Figure 1.

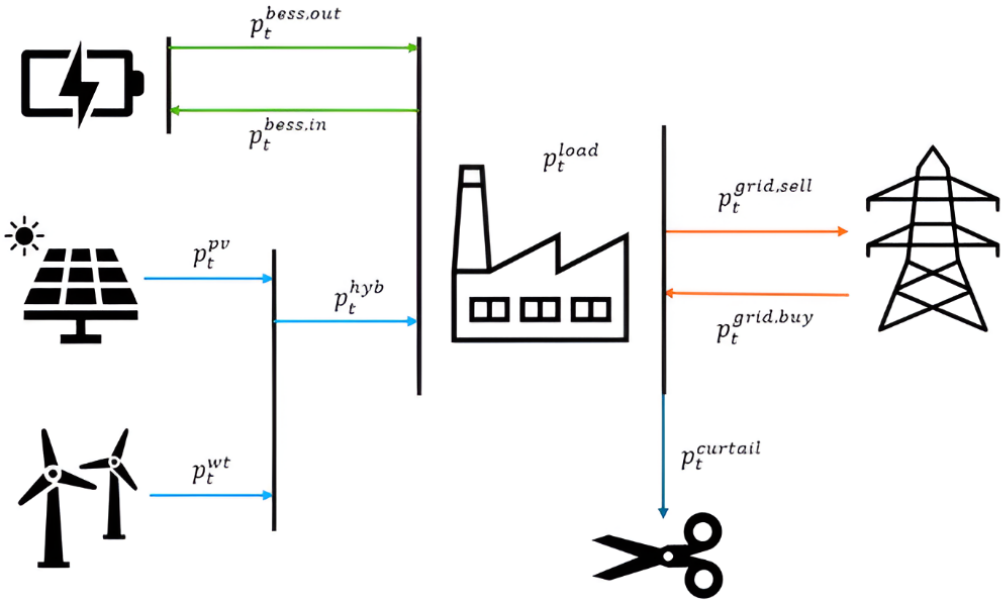

Figure 1. Scheme of the system analyzed.

2.1. Deterministic Mathematical Formulation

This problem was modeled as a single-objective MILP. The objective function chosen is the Net Present Cost, calculated as the sum of the discounted present costs minus the discounted present incomes through the useful lifetime of the system [36], considering also the investment costs applied at the year "zero". The simulation is done throughout a one-year horizon, and the savings found are then actualized for each year of the life cycle to compute the NPC. The complete expression is presented in Equation (2), which is minimized in the optimization process.

$$\min \quad NPC = \sum_{y=1}^{years} \left(\frac{Annual\ Costs_y - Revenues_y}{(1+r)^y} \right) + Investment\ Costs \tag{2}$$

$$Annual\ Costs_y = C^{en,grid} \cdot \sum_{t=1}^{8760} p_t^{grid,buy} + OPEX^{wt} \cdot x^{wt} + OPEX^{pv} \cdot x^{pv} + OPEX^{bess} \cdot x^{bess} \tag{3}$$

$$Revenues_y = \sum_{t=1}^{8760} (p_t^{grid,sell} \cdot PZ_t) \tag{4}$$

$$Investment\ Costs = CAPEX^{wt} \cdot x^{wt} + CAPEX^{pv} \cdot x^{pv} + CAPEX^{bess} \cdot x^{bess} \tag{5}$$

Equation (3) includes all the costs that the system must sustain annually: the OPEX of the various elements, expressed as €/MW (or €/MWh), and the expenditures to purchase the residual energy required from the grid. Excess energy can be sold at the zonal price, resulting in a positive income, computed in Equation (4). Finally, in Equation (5) are reported the investment costs of the three elements of the system, which will be accounted for at year zero. The CAPEX are expressed as €/MW (or €/MWh).

The energy balance ensures that power demand is satisfied for each time step through renewable generation, storage operation, and grid exchanges. This constraint is expressed in Equation (6).

$$p_t^{hyb} + p_t^{grid,buy} + p_t^{bess,out} = D_t + p_t^{grid,sell} + p_t^{bess,in} + p_t^{curtail} \tag{6}$$

For each time stamp, the system can only buy or sell energy with the grid; this behavior is controlled using two binary variables $y_t^{grid,buy}$, $y_t^{grid,sell}$ modeled with Equations (7) and (8), where $i \in \{buy, sell\}$.

$$p_t^{grid,i} \leq P_{max}^{grid} \cdot y_t^{grid,i} \tag{7}$$

$$p_t^{grid,i} \geq 0 \tag{8}$$

$$y_t^{grid,sell} + y_t^{grid,buy} \leq 1 \tag{9}$$

Equations (7) and (8) are modeled using the big-M constraint [37], by selecting the maximum power (P_{max}^{grid}) that can be withdrawn or taken from the grid as the big-M constant. Equation (9) is the one that ensures that for each time instant, it is only possible to buy or to sell. $p_t^{curtail}$ represents the over-generation power that must be curtailed to not exceed the grid limit. To ensure realistic operating conditions, the ratio between the energy curtailed and the total energy produced is limited to a maximum value, as defined in Equation (10). This equation is nonlinear; to linearize it, it can be rewritten as reported in Equation (11).

$$\frac{\sum_{t=1}^{8760} p_t^{curtail}}{\sum_{t=1}^{8760} p_t^{hyb}} \leq E_{max}^{curtail} \tag{10}$$

$$\sum_{t=1}^{8760} p_t^{curtail} - E_{max}^{curtail} \cdot \sum_{t=1}^{8760} p_t^{hyb} \leq 0 \tag{11}$$

$p_t^{bess,out}$, $p_t^{bess,in}$ are the power exchanged with the BESS; they are also modeled using the big-M constraint [37] to ensure that the battery can only be charged (or discharged) for each time interval, using a binary variable (y_t^{bess}) with Equations (12) and (13).

$$p_t^{bess,in} \leq (1 - y_t^{bess}) \cdot M \tag{12}$$

$$p_t^{bess,out} \leq y_t^{bess} \cdot M \tag{13}$$

Constraints (14) and (15) limit the amount of power that can be exchanged within the BESS, which is dependent on the capacity (x^{bess}), and on the Energy-to-Power Ratio (EPR). This value represents the duration of the battery, or the hours that the battery can sustain its maximum capacity before being fully discharged.

$$0 \leq p_t^{bess,in} \leq \frac{1}{EPR} \cdot x^{bess} \tag{14}$$

$$0 \leq p_t^{bess,out} \leq \frac{1}{EPR} \cdot x^{bess} \tag{15}$$

The State Of Charge (SOC) of the BESS is calculated with Equation (16) using a constant efficiency (η^{bess}) model. Its maximum value is limited by the BESS capacity with constraint (17).

$$soc_t = p_t^{bess,in} \cdot \eta^{bess} - \frac{p_t^{bess,out}}{\eta^{bess}} + soc_{t-1} \tag{16}$$

$$0 \leq soc_t \leq x^{bess} \tag{17}$$

In the proposed model, one of the most important assumption rules that the BESS can interact only with the load to avoid the possibility of doing arbitrage with the grid, by charging/discharging with the energy bought/sold from the grid. To ensure this behavior, the binary variables previously defined are constrained in Equation (18). In particular, this choice was made to show the contribution that BESS can have to increasing the self-consumption of the energy produced, avoiding additional economic benefits from grid interaction.

$$y_t^{bess} + y_t^{grid,sell} \leq 1 \tag{18}$$

The main goal of the sizing procedure is to maximize the share of renewable sources. For this reason, as Key Performance Index (KPI), a reliability index can be computed, in particular, the Energy Not Served (ENS), defined as the load share not fed by renewables, including the energy storage support, over one year, is computed in Equation (19).

$$ENS = 1 - \frac{\sum_{t=1}^{8760}(p_t^{hyb} + p_t^{bess,out} - p_t^{grid,sell} - p_t^{bess,in} - p_t^{curtail})}{\sum_{t=1}^{8760} D_t} \tag{19}$$

2.2. Robust Mathematical Formulation

In this study, two sources of uncertainty are considered: the zonal energy price and the load demand. It follows that the deterministic problem must be reformulated in a robust model.

The uncertainty of the energy price is formulated based on the model proposed by Mojtaba et al. [31]: since the energy sold by the system will create a positive income to the NPC, coherently within the worst-case scenario, the uncertainty must cause a reduction of the revenues, therefore the price should be lower compared to the no-uncertainty scenario. This effect is achieved by an additional term introduced in Equation (4), leading to the new robust formulation reported in Equation (20). To treat the robust formulation in a linear form, the strong duality theory must be applied [38]. The variables ζ_t^{price} and

β^{price} are the dual variables used to model the uncertainty; they can be controlled using Equation (21) [31].

$$Revenues_y = \sum_{t=1}^{8760}(p_t^{grid,sell} \cdot PZ_t) - (\sum_{t=1}^{8760} \xi_t^{price} + \beta^{price} \cdot \Gamma^{price}) \quad (20)$$

$$\xi_t^{price} + \beta^{price} \geq \Delta PZ_t \cdot p_t^{grid,sell} \quad (21)$$

The term ΔPZ_t is a parameter that expresses the maximum deviation that the zonal price can have for each time interval. The parameter Γ^{price} is also called uncertainty budget and is used to control the level of robustness expected in the solution. It represents the amount of uncertainty that the solver can spend through the time period considered. In the optimization process, the solver will distribute the uncertainty available to reach the worst case, based on all the other conditions of the system. Specifically, the uncertainty budget is the number of hours for which it is possible to have the maximum deviation. For example, with a Γ = 50%, which over one year is equivalent to 4380 h, it is possible to have 4380 h with the maximum deviation and the remaining with zero deviation (according to the definition given of uncertainty budget); or it can be split through all the hours with different levels. It is important to highlight that the way the uncertainty is divided is based on the overall operating condition of the system, i.e., it is not stochastic.

The second source of uncertainty considered, the load demand, affects the energy balance of the system, which is changed to its new formulation defined in Equation (22).

$$p_t^{hyb} + p_t^{grid,buy} + p_t^{bess,out} = (D_t + \xi_t^{load} + \beta^{load} \cdot \Gamma^{load}) + p_t^{grid,sell} + p_t^{bess,in} + p_t^{curtail} \quad (22)$$

At the nominal demand, D_t, is added the robust uncertainty term, once again composed of the two dual variables, and the uncertainty budget. In this case, the uncertainty will cause an increase in the total demand. The uncertainty budget associated with the load (Γ^{load}) is expressed as a percentage varying between 0 and 100%. On the contrary, the uncertainty budget related to the price (Γ^{price}) is expressed, as stated before, in hours and can vary between 0 and 8760. Despite the two different formulations, both parameters represent the amount of uncertainty that can be present over the time horizon considered. The correct behavior of the dual variables is ruled by Equations (23) and (24).

$$\xi_t^{load} + \beta^{load} \geq \Delta D_t \quad (23)$$

$$\xi_t^{load} + \beta^{load} \cdot \Gamma^{load} \leq \Delta D_t \quad (24)$$

The load demand is also present in Equation (19) that will be modified by adding its relative uncertainty, as defined in Equation (25).

$$ENS = 1 - \frac{\sum_{t=1}^{8760}(p_t^{hyb} + p_t^{bess,out} - p_t^{grid,sell} - p_t^{bess,in} - p_t^{curtail})}{\sum_{t=1}^{8760}(D_t + \xi_t^{load} + \beta^{load} \cdot \Gamma^{load})} \quad (25)$$

3. Study Case and Methods

3.1. Study Case

To validate the proposed model, a synthetic case study has been adopted, which is relevant to an industrial load located in the south of Italy, in particular in the Puglia region. As reported in [39], this region is crucial for Italian wind energy, since it exhibits the highest potential installable wind power while requiring a limited occupation of regional land area. In addition, as for all the southern region of the Italian peninsula, it also has a relevant amount of solar potential, with a production between 1400–1500 kWh/kW/year [40].

Given the wind and PV potential, this region is a perfect candidate for the HRES model under investigation.

The PV generation data were obtained from the software PVsyst v8.0.0 using meteorological data that can be found on the database Solargis Prospect [41]. The data of WT production were taken from [42]. The load demand is derived from the ELMAS database [43], the load chosen presents the consumption characteristics of an industrial site: constant consumption during the working hours, with a reduction during the night. A higher reduction is present during the weekends and during Christmas and the summer vacation periods. Since the plant can interact with the grid, zonal price data are needed. The distribution price corresponding to southern Italy was taken from the Ember dataset [44].

Considering all the other parameters presented in Section 2, their values and sources are reported in Table 1. It is relevant to stress that the CAPEX (and consequently the OPEX) of the BESS are a function of the EPR. The life cycle of the plant was set to 25 years.

Table 1. Input data summary.

Parameter	Unit	Value	Source
years	-	25	assumption
$CAPEX^{wt}$	€/MW	1,325,000	[45]
$CAPEX^{pv}$	€/MW	700,000	[46]
$CAPEX^{bess}$	€/MWh	$220 \cdot EPR^{-0.9795} + 287.1$	[47]
$OPEX^{wt}$	€/MW	14,575	[45]
$OPEX^{pv}$	€/MW	6100	[46]
$OPEX^{bess}$	€/MWh	2.5% of CAPEX	[47]
$C^{en,grid}$	€/MWh	200	assumption
r	%	5	assumption
P_{max}^{grid}	MW	150	assumption
$E_{max}^{curtail}$	%	3	assumption
η^{bess}	%	95	assumption
EPR	h	3 or 4	computed

3.2. Methods

Simulations were done over a full-year horizon with an hourly time step, using Gurobi as optimization solver. Accordingly, a one-year time series with hourly resolution was derived from the dataset presented in the previous subsection. Production profiles of PV and WT are normalized to a 1 MW capacity plant, which will be scaled by the corresponding design variables that represent the installed capacities of the two technologies. The load demand data were scaled down by a factor of four to obtain more realistic values compatible with the considered renewable generation unit.

The zonal price is the only dataset composed of multiple years. Since a single representative year is required, a statistical approach was used. The average price was computed for each month across the available years; these monthly values were then compared, and the median one was identified; the hourly zonal price corresponding to this median month was then selected and used as the representative month in the construction of the typical price.

Figure 2 reports the input data profiles, where thin gray lines represent individual weekly profiles, while the thick colored line depicts the average weekly behavior.

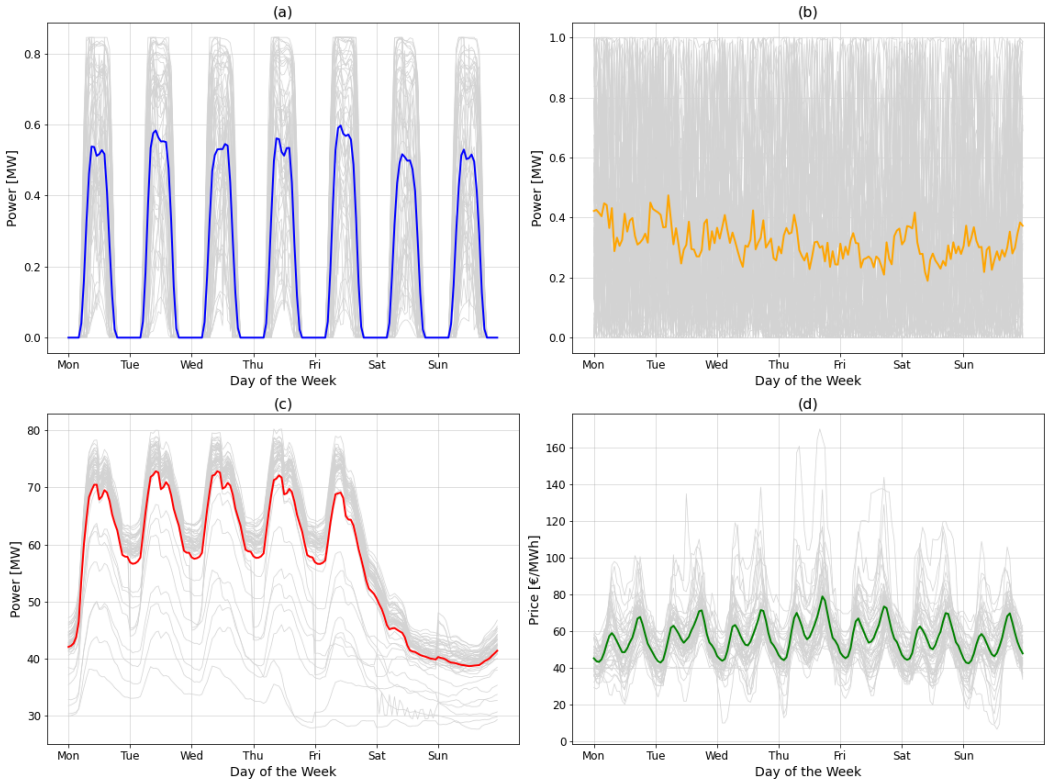

Figure 2. Behavior of the input data considered for this study: (**a**) PV generation, (**b**) WT generation, (**c**) Load, (**d**) PZ.

Finally, for load demand and zonal price, a deviation vector (ΔD_t, ΔPZ_t) is also required for the robust formulation. For simplicity, it is modeled as a percentage variation of the deterministic data value. In this analysis, a maximum hourly deviation of 10% is assumed.

Different scenarios were defined and simulated to explore different configurations of the plant, as reported in Table 2. Scenario 1 and Scenario 2 consider only one renewable resource at a time to show the need for hybridization, which is simulated with Scenario 3, where the two RES are combined. In Scenario 4, BESS is added to further increase the penetration of renewable, in this case, the BESS is allowed to exchange energy only with the load. The EPR for this scenario is equal to 3 h, which was found as the optimal value that minimizes the NPC, as discussed in Section 4. Finally, an additional Scenario 5 was defined to evaluate the effect on the KPIs when the BESS is allowed to also sell energy to the grid. In this case, the optimal EPR found and then used was 4 h. These scenarios aim to show the benefits of hybridization when dealing with RES, with particular attention to the positive effect of BESS. But also to show what happens to the solution when uncertainty is considered, and if particular configurations can reduce the effect that uncertainty has on the sizing optimization.

Table 2. Summary of the different scenarios compared in this study.

Scenario	WT	PV	BESS	BESS to Grid
1	✓			
2		✓		
3	✓	✓		
4	✓	✓	✓	
5	✓	✓	✓	✓

4. Results and Discussion

In this section, the main results are presented and discussed. Initially, the simulations were done for the deterministic case, so when no uncertainty is considered. Then, the uncertainty is added into the simulations, and a sensitivity analysis was conducted to show the robustness of different plant configurations. All the simulations were carried out on a 3 GHz Intel i9-10980XE computer with 128 GB of RAM. The KPIs used for the comparison are the NPC and the ENS, to give both an economic and a reliability analysis.

4.1. Deterministic Optimization Results

The deterministic analysis is essential to define a benchmark case, i.e., a scenario in which no uncertainty is considered. This represents the starting point to highlight the benefits of hybridization, with particular attention to the industrial case study under analysis. The results of these simulations are reported in Table 3.

Table 3. Summary of the results of the deterministic optimization.

Scenario	WT [MW]	PV [MW]	BESS [MWh]	NPC [M€]	ENS [%]
1	237.5	-	-	621.61	36.69
2	-	284.64	-	782.61	56.23
3	192.5	170.32	-	397.38	22.29
4	205	210.15	193.75	320.57	8.3
5	225	222.43	269.98	296.76	5.49

It is important to underline that for the two scenarios involving a BESS, the optimal EPR considered was computed by launching multiple simulations with different EPR values and selecting the one that minimizes the NPC. The results of this procedure are shown in Figure 3, an EPR of 3 h is adopted for Scenario 4 and an EPR of 4 h for Scenario 5. This behavior is due to the fact that the EPR affects not only the BESS model but especially its costs. The CAPEX were computed using an exponential function presented in [47], according to which higher EPR values correspond to lower costs. Therefore, intermediate EPR values seem to be the best trade-off between reduced costs and BESS size. The variability of the solution observed in Figure 3 makes clear the importance of the EPR as sizing parameter when dealing with BESS. A range of profitable EPR can be identified: 3–4 h for Scenario 4 and 2–4 h for Scenario 5. Outside of these ranges, the NPC increases significantly.

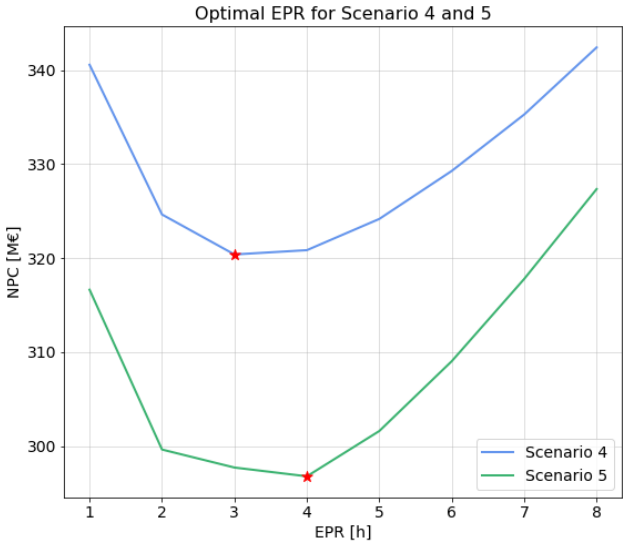

Figure 3. Optimal EPR analysis, red stars represent the minimum point of the curve.

From Table 3 emerges that when a single RES is considered, both ENS and NPC are high, in particular, this is more relevant in the only PV configuration (Scenario 2). This is due to the load profile considered, which shows a significant demand during the nighttime (just below 60 MW during weekdays); for this reason, WT is a more suitable resource and has the best impact on the energy demand satisfied, which is 20% higher compared to the only PV scenario. This is also confirmed by the equivalent hours, which are 2788 for WT and 1866 for PV. The combination of WT and PV (Scenario 3) improves the solution from both the economic and the reliability point of view, with a reduction of the NPC of around 36% compared to the single WT scenario and of 49.22% compared to the single PV scenario. This behavior can be observed in the energy balance diagrams reported in Figure 4. Although the simulation life span is a whole year, a single weekday is depicted. When a single source is present, Figure 4a,b, energy production cannot be controlled: when energy is generated, it is either consumed by the load or, if in excess, sold to the grid or curtailed. When both WT and PV are included, Figure 4c, a greater portion of the energy demand can be met, thereby reducing the amount of energy purchased from the grid. Considering the operational cost of a year, the reduced dependence on the grid through the life cycle makes the configuration more profitable, although with a higher initial investment cost.

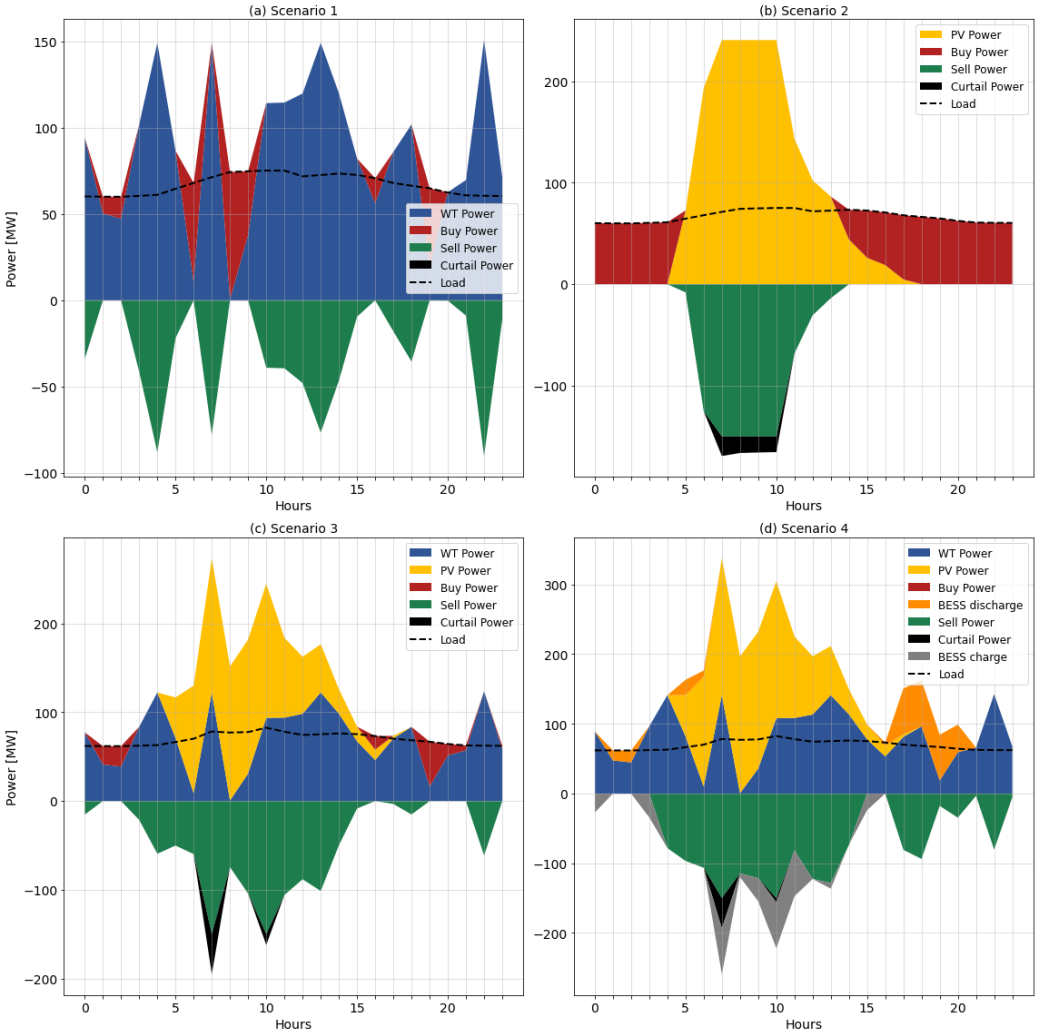

Figure 4. Energy balance comparison between Scenario 1, 2, 3, and 4.

The most significant improvement is achieved when a BESS is added to the system, leading to an ENS lower than 10% and a substantial reduction of the NPC. As shown in Figure 4d, the load can be completely satisfied by the renewable plant without buying

energy from the grid. The situation can be further improved when the BESS is allowed to sell energy to the grid; thanks to this additional chance, the RES size can be increased since it is lower the amount of energy that must be curtailed. Consequently, both economic and reliability performance are better, reaching a system that is almost completely disconnected from the grid.

A comparison of the economic performance between all scenarios is reported in Figure 5, the value related to the CAPEX are accounted at year zero, while OPEX and revenues are evaluated through the life cycle of the plant. Scenario 2 can be identified as the one 'OPEX-intensive' since it presents the highest operational costs, mainly related to energy bought from the grid. Vice versa, Scenario 5 is the one 'CAPEX-intensive', for the highest CAPEX between the configurations, but also the one capable of generating more profit. This diagram shows, once again, the importance of hybridization, also from the economic point of view. Although CAPEX increase, the significant reduction of the OPEX and the increase in revenues make the hybridization investment more profitable.

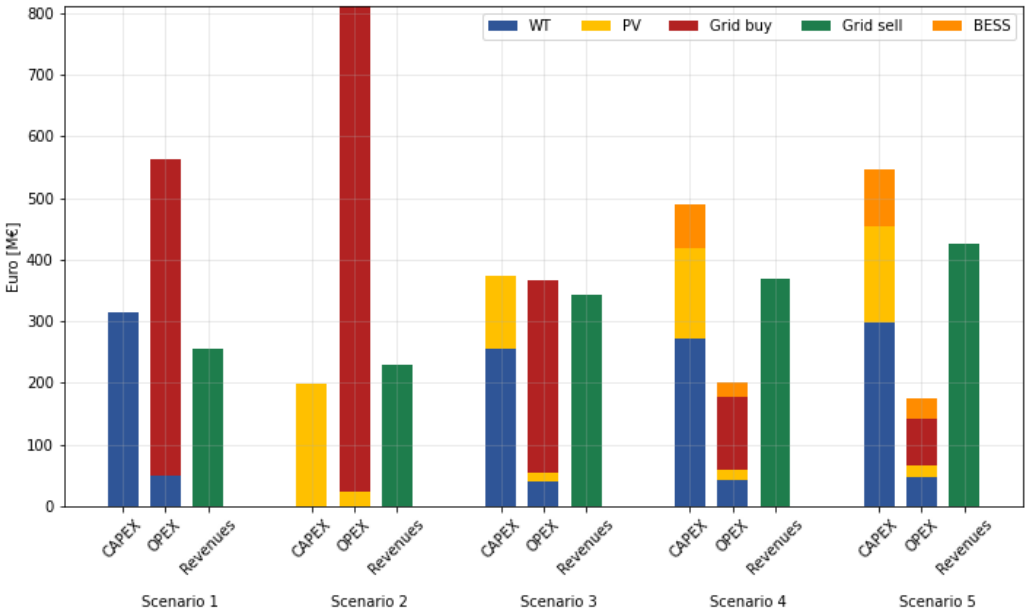

Figure 5. Economics analysis between all scenarios.

Regarding the computational effort, configurations including a single RES require 2.5 s per simulation, while when both WT and PV are considered, the computational time increases to about 4 s. The situation changes meaningfully when a BESS is added to the system. The total number of variables (both continuous and integer) increases by 40%, leading to a computational time of 62 s for Scenario 4. This is consistent with the exponential growth in solution time associated with MILP problems when the number of variables increases. In Scenario 5, the possibility of BESS to interact with the grid simplifies the model since there is no Equation (18) that involves two binary variables, reducing the time required by one simulation to 15 s and making the problem more tractable.

4.2. Uncertainty Sensitivity Analysis

The uncertainty is then added to the model. A sensitivity analysis was conducted by varying both the uncertainty budget of load (Γ^{load}) and price (Γ^{price}). The values that this parameter can assume are different based on the two different models applied. For the load, it is expressed as a percentage that was varied between 0 and 100%; vice versa, for the price, it is expressed as a number of hours, as already pointed out in Section 2, and it was varied between 0 and 8760. Thus, for both the uncertainty, the effect was studied between

the deterministic case and the maximum uncertainty case. The simulations were done for Scenario 3 and Scenario 5 to check the different effects on a simple hybrid plant, and on one that includes a BESS. Scenario 5 was chosen over Scenario 4 for computational time reasons, since it is much faster and more suitable for sensitivity analysis when several simulations must be run. This aspect is particularly relevant as the uncertainty significantly impacts the computational effort. In particular, a simulation for Scenario 3 runs in 11.38 s, an increase of almost 3 times compared to the deterministic case, while for Scenario 5 it reaches 46.50 s, again more than 3 times higher. The EPR of Scenario 5 was maintained at a constant of 4 h, see Figure 3.

The NPC obtained from the sensitivity analysis is reported in Figure 6. It can be observed that the configuration including a BESS is always better compared to a simple HRES. The increase in NPC is lower when a BESS is present; thus, the system is more robust with respect to uncertainty. This trend is true except at very high values of uncertainty, for which the increase in NPC is more pronounced. This can be explained by the fact that in these simulations, the EPR was fixed at the constant optimal value for the deterministic case, which may no longer be optimal under uncertainty. This issue will be dealt with in the following subsection. Another important outcome is that the price uncertainty has a higher impact than the load uncertainty. This is connected with the fact that the price uncertainty directly affects the objective function, or the NPC.

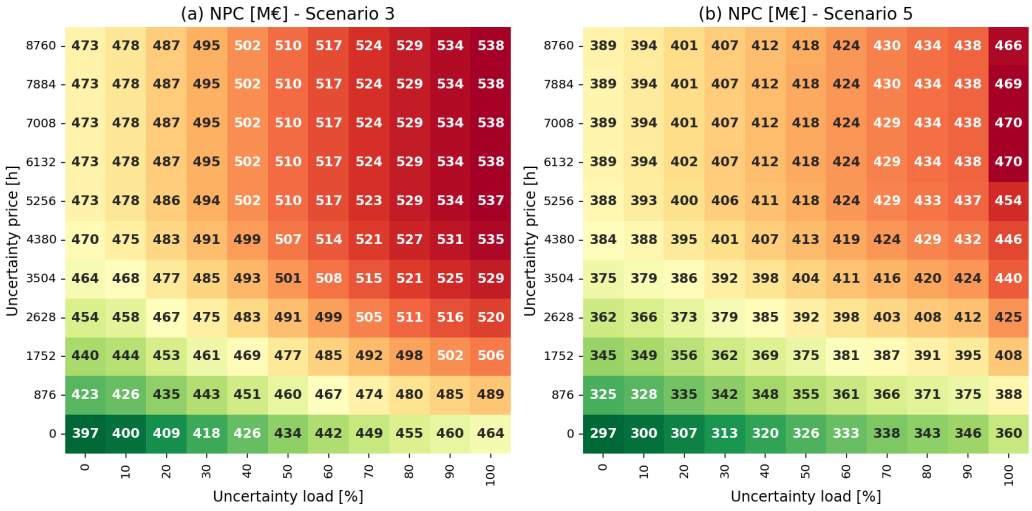

Figure 6. Heat map of NPC for Scenario 3 and Scenario 5.

Finally, it is interesting to notice that, once a certain value of Γ^{price} is reached, which is variable depending on the HRES scenario and on the load uncertainty value, the NPC becomes constant. To deeply understand this behavior, it is crucial to have a clear understanding of what the uncertainty budget represents. As already explained in Section 2, this parameter expresses the amount of uncertainty that is possible to spend through the time period analyzed. Considering the uncertainty of the zonal price, from Equation (21), emerges that the deviation is defined only in the hours during which the system is selling energy to the grid. Hence, the solver will start to allocate the uncertainty during these hours to reach the worst-case scenario. As soon as they are all saturated, the uncertainty will be assigned to the remaining hours, but this will not cause any reduction to the NPC since there are no grid revenues during that hour. Thus, once the uncertainty budget reaches the value equivalent to the amount of selling hours, even if it is further increased, there will not be any effect on the objective function, resulting in a constant NPC value.

4.3. Uncertainty and EPR Sensitivity Analysis

As previously mentioned, the EPR used in the uncertainty sensitivity analysis was kept constant at a value of 4 h, see Figure 3. Thus, it is the one obtained for the deterministic optimization, and not specific to the uncertainty case. For this reason, the sensitivity described in the previous subsection has been extended over a wider range of EPR values; in particular, a range between 1 and 8 has been investigated, since these are the typical values found in the literature to capture a wide range of operating conditions.

Each uncertainty level was simulated eight times by varying the EPR; among all of them, the configuration that minimizes the NPC was selected. The optimal NPC heat-map obtained is reported in Figure 7a.

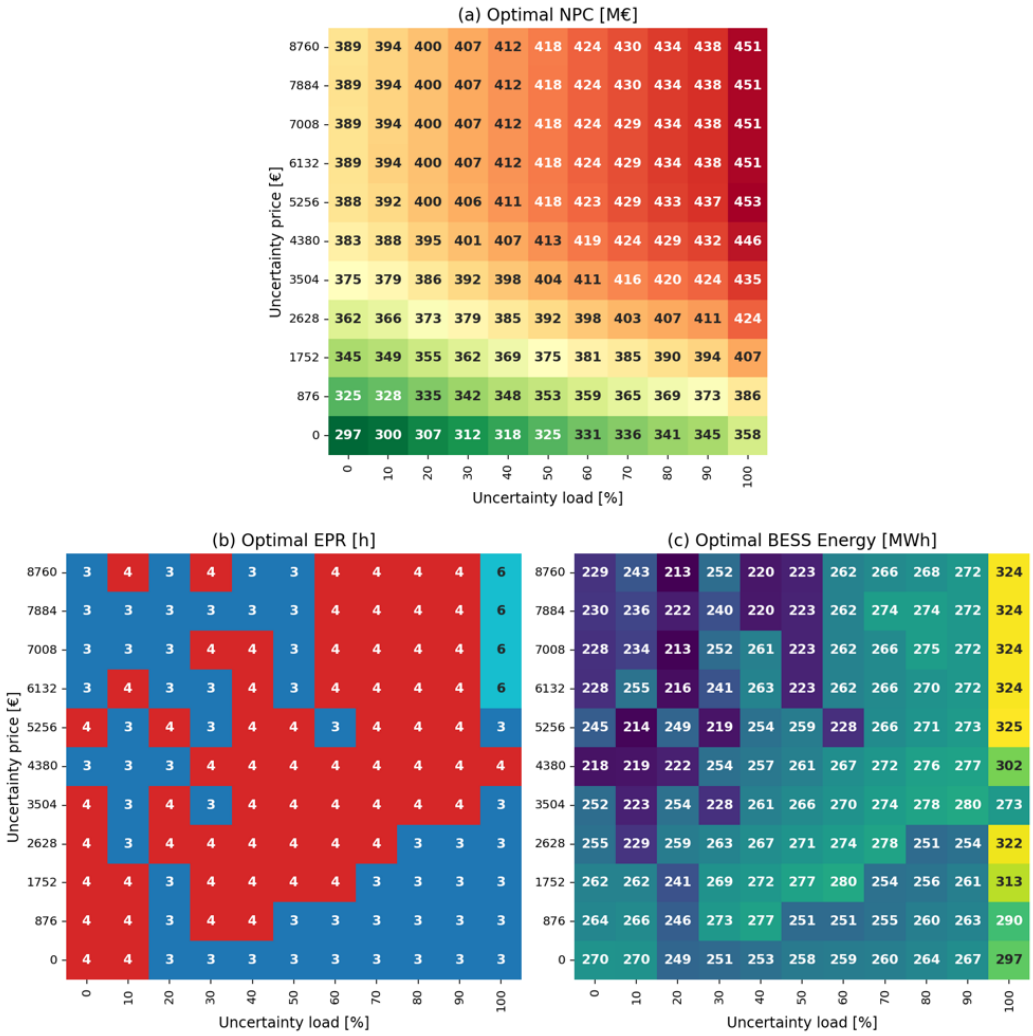

Figure 7. Heat map of the optimal NPC (**a**), EPR (**b**), and BESS energy (**c**) with variable uncertainty.

Once the minimum NPC is identified, it becomes possible to determine the relative values of EPR and BESS energy to assess the optimal BESS size capable of ensuring the highest system robustness. The results are shown in Figure 7b,c. Although an EPR of 4 h is still the predominant value, in a significant number of cases, an EPR of 3 h can help to reduce the NPC. For very high uncertainties in both load and price, a high BESS duration results in a more robust system to uncertainty; in particular, the optimal EPR resulted in an equal value of 6 h. A high uncertainty level of the load increases the mismatches between generation and demand; thus, a greater energy buffering capability is needed. In these

conditions, a BESS with higher EPR allows to sustain energy exchanges for longer periods, increasing the robustness of the system.

4.4. Results Comparison with the Literature

A comparison with recent robust optimization studies is reported in Table 4. Different robust approaches were analyzed, including Adaptive Robust Optimization (ARO), Affinely Adjustable Robust Optimization (AARO), proposed Robust Optimization (RO) MILP approach. The comparison focuses on the reliability index and computational time. The result shows that the proposed approach can ensure competitive reliability performance while maintaining a comparable computational time with other advanced robust formulation approaches.

Table 4. Results comparison with the literature.

Reference	Method	Reliability	Simulation Time [s]
[34]	ARO MILP	Unmet Demand = 18.7%	56.6
[48]	AARO MILP	Unserved Energy = 0 kWh	48
Proposed approach	RO MILP	ENS = 6.42%	46.5

5. Conclusions and Future Developments

The hybridization of renewable resources represents a key element in the transition toward green power generation. Understanding how different technologies can be combined is essential to achieving production profiles that are similar to those of conventional fossil fuel systems. In this study, a MILP optimization model was developed to support the design of HRES under multiple sources of uncertainty. The approach used to model the uncertainty represents a good solution to maintain a tractable linear problem that can be solved using a MILP, ensuring the optimal solution.

The results demonstrate that hybridization (Scenario 3) can reduce the NPC of HRES by up to 50% compared to single-technology configurations, while also improving the reliability with a larger amount of satisfied load. A BESS can increase the overall performance and guarantee a higher robustness when uncertainty is considered. In particular, BESS sizing requires a proper consideration of both energy (or power) and duration. From the preliminary sensitivity on EPR, it is shown that EPR has an impact on the profitability of the system, with an NPC that can be 10% higher compared to the optimal one. This is more evident when the optimal EPR for the different uncertainty combinations is computed. The heat-map obtained shows that for a high level of uncertainty, higher values of duration can be useful to obtain a restrained NPC.

Regardless of the promising results obtained, the model presents some limitations that must be highlighted. Firstly, the uncertainty associated with RES was not considered. This assumption was made to maintain a tractable linear formulation, since the robust modeling of RES uncertainty creates non-linear equations. However, renewable variability represents a relevant source of uncertainty in HRES and should be integrated in future developments to provide a more complete robustness analysis. Due to the significant role of the BESS, it is important to underline that a simple battery model was considered in this study, assuming constant efficiency and no calendar or cycle aging over time. Battery degradation strongly affects the economics and sizing of storage systems, particularly with a long-term time horizon. Therefore, future developments should include more realistic degradation BESS models capable of accounting for capacity fade and efficiency variations over time. In this work, the EPR was analyzed with a sensitivity-based approach instead of being directly optimized in the MILP formulation. This choice was motivated by the non-linear relations between EPR and BESS capacity, particularly in Equations (14) and (15),

which would prevent maintaining a MILP formulation. Future research could investigate linear approximation techniques or two-stage optimization methods to include EPR as a decision variable in the model. These future developments will inevitably increase the computational complexity of the problem. This issue could be managed by introducing a temporal reduction technique capable of reducing the simulation time while maintaining the system dynamics. Other optimization techniques could also be studied and added, such as multi-objective optimization, Pareto-front analysis, and the Modeling to Generate Alternatives (MGA).

This tool can represent a strong foundation for the future development of a more advanced solver, capable of handling the complexities of integrating renewable energy into the national power system, enabling the achievement of the decarbonization target. This will be fundamental to sustain the transition process, which will interest the energy world in the coming years.

Author Contributions: Conceptualization, T.D., C.M.C., M.S. and M.M.; methodology, T.D. and C.M.C.; software, T.D. and C.M.C.; validation, T.D., C.M.C. and M.M.; formal analysis, T.D.; investigation, T.D., C.M.C. and M.M.; resources, T.D. and M.M.; data curation, T.D.; writing—original draft preparation, T.D. and C.M.C.; writing—review and editing, T.D., M.S. and M.M.; visualization, T.D.; supervision, M.M.; project administration, M.M. All authors have read and agreed to the published version of the manuscript.

Funding: This research received no external funding.

Data Availability Statement: The data are contained within the article.

Conflicts of Interest: The authors declare no conflicts of interest.

Abbreviations

The following abbreviations are used in this manuscript:

AARO	Affinely Adjustable Robust Optimization
ARO	Adaptive Robust Optimization
BESS	Battery Energy Storage System
ENS	Energy Not Served
ES	Energy Served
EPR	Energy-to-Power Ratio
HRES	Hybrid Renewable Energy System
KPI	Key Parameter Index
LOLP	Loss Of Load Probability
MILP	Mixed-Integer Linear Programming
NPC	Net Present Cost
NPV	Net Present Value
PV	Photovoltaic Panels
PZ	Zonal Price
RES	Renewable Energy Sources
RO	Robust Optimization
SOC	State Of Charge
WT	Wind Turbine

Nomenclature

The following nomenclature is employed in this manuscript:

Sets:

$\mathcal{T}$/t	Set and index for time steps
$\mathcal{Y}$/y	Set and index for years

Design Variables:	
x^{wt}	Number of WT
x^{pv}	Capacity of PV [MW]
x^{bess}	Capacity of BESS [MWh]
Control Variables:	
p_t^{hyb}	Combined power WT e PV [MW]
$p_t^{bess,in}$	Charging power [MW]
$p_t^{bess,out}$	Discharging power [MW]
$p_t^{grid,sell}$	Power sell to the grid [MW]
$p_t^{grid,buy}$	Power buy from the grid [MW]
$p_t^{curtail}$	Over-generation curtailed power [MW]
soc_t	State of charge [MWh]
y_t^{bess}	Binary for BESS
$y_t^{grid,sell}$	Binary for grid sell
$y_t^{grid,buy}$	Binary for grid buy
ξ_t^{load}	Dual variable load 1 [MW]
β^{load}	Dual variable load 2 [MW]
ξ_t^{price}	Dual variable price 1 [€]
β^{price}	Dual variable 2 [€]
Parameters:	
P_t^{wt}	Production of 1 WT [MW]
P_t^{pv}	Production of 1 MW of PV [MW]
D_t	Load demand [MW]
PZ_t	Zonal price [€/MWh]
$CAPEX^{wt}$	CAPEX of WT [€/MW]
$CAPEX^{pv}$	CAPEX of PV [€/MW]
$CAPEX^{bess}$	CAPEX of BESS [€/MWh]
$OPEX^{wt}$	OPEX of WT [€/MW]
$OPEX^{pv}$	OPEX of PV [€/MW]
r	Discount rate [%]
P_{max}^{grid}	Maximum power at the grid [MW]
$E_{max}^{curtail}$	Maximum curtailment allowed [%]
η^{bess}	Efficiency of the BESS [%]
EPR	Energy to power ratio of BESS [h]
N_{max}^{wt}	Maximum number of WT
N_{max}^{pv}	Maximum capacity of PV [MW]
N_{max}^{bess}	Maximum capacity of BESS [MWh]
ΔD_t	Max deviation of load demand [MW]
ΔPZ_t	Max deviation of PZ [€/MWh]
Γ^{load}	Uncertainty budget of load [%]
Γ^{price}	Uncertainty budget of price [h]

References

1. IEA. *World Energy Outlook 2025*; Technical Report; IEA: Paris, France, 2025.
2. Ember. *Global Electricity Review 2025*; Technical Report; Ember: London, UK, 2025.
3. Ren21. *Renewables 2025 Global Status Report*; Technical Report; Ren21: Paris, France, 2025.
4. BloombergNEF. *New Energy Outlook 2025*; Technical Report; BloombergNEF: New York, NY, USA, 2025.
5. Krishna, K.S.; Kumar, K.S. A review on hybrid renewable energy systems. *Renew. Sustain. Energy Rev.* **2015**, *52*, 907–916. [CrossRef]
6. Deshmukh, M.K.; Deshmukh, S.S. Modeling of hybrid renewable energy systems. *Renew. Sustain. Energy Rev.* **2008**, *12*, 235–249. [CrossRef]
7. Bassey, K.E. Hybrid renewable energy systems modeling. *Eng. Sci. Technol. J.* **2023**, *4*, 571–588. [CrossRef]

8. Bajpai, P.; Dash, V. Hybrid renewable energy systems for power generation in stand-alone applications: A review. *Renew. Sustain. Energy Rev.* **2012**, *16*, 2926–2939. [CrossRef]
9. Sinha, S.; Chandel, S.S. Review of software tools for hybrid renewable energy systems. *Renew. Sustain. Energy Rev.* **2014**, *32*, 192–205. [CrossRef]
10. Khan, A.A.; Minai, A.F.; Pachauri, R.K.; Malik, H. Optimal Sizing, Control, and Management Strategies for Hybrid Renewable Energy Systems: A Comprehensive Review. *Energies* **2022**, *15*, 6249. [CrossRef]
11. Lian, J.; Zhang, Y.; Ma, C.; Yang, Y.; Chaima, E. A review on recent sizing methodologies of hybrid renewable energy systems. *Energy Convers. Manag.* **2019**, *199*, 112027. [CrossRef]
12. Sakki, G.K.; Tsoukalas, I.; Kossieris, P.; Makropoulos, C.; Efstratiadis, A. Stochastic simulation-optimization framework for the design and assessment of renewable energy systems under uncertainty. *Renew. Sustain. Energy Rev.* **2022**, *168*, 112886. [CrossRef]
13. International Renewable Energy Agency. *Advanced Forecasting of Variable Renewable Power Generation: Innovation Landscape Brief*; IRENA: Abu Dhabi, United Arab Emirates, 2020.
14. Hodge, B.M.; Ela, E.; Milligan, M. *The Distribution of Wind Power Forecast Errors from Operational Systems*; Technical Report; NREL: Golden, CO, USA, 2011.
15. González, A.; Riba, J.R.; Rius, A.; Puig, R. Optimal sizing of a hybrid grid-connected photovoltaic and wind power system. *Appl. Energy* **2015**, *154*, 752–762. [CrossRef]
16. Chen, H.C. Optimum capacity determination of stand-alone hybrid generation system considering cost and reliability. *Appl. Energy* **2013**, *103*, 155–164. [CrossRef]
17. Akram, U.; Khalid, M.; Shafiq, S. Optimal sizing of a wind/solar/battery hybrid grid-connected microgrid system. *IET Renew. Power Gener.* **2018**, *12*, 72–80. [CrossRef]
18. Lamedica, R.; Santini, E.; Ruvio, A.; Palagi, L.; Rossetta, I. A MILP methodology to optimize sizing of PV - Wind renewable energy systems. *Energy* **2018**, *165*, 385–398. [CrossRef]
19. Dufo-López, R.; Bernal-Agustín, J.L. Multi-objective design of PV-wind-diesel-hydrogen-battery systems. *Renew. Energy* **2008**, *33*, 2559–2572. [CrossRef]
20. Giedraityte, A.; Rimkevicius, S.; Marciukaitis, M.; Radziukynas, V.; Bakas, R. Hybrid Renewable Energy Systems—A Review of Optimization Approaches and Future Challenges. *Appl. Sci.* **2025**, *15*, 1744. [CrossRef]
21. Choi, S.; Cho, K. A Scenario-Based Approach to Using Electric Vehicle Batteries in Virtual Power Plants: Insights from Environmental, Social, and Governance and Monte Carlo Simulations. *Sustainability* **2025**, *17*, 3224. [CrossRef]
22. Bhandari, B.; Lee, K.T.; Lee, G.Y.; Cho, Y.M.; Ahn, S.H. Optimization of Hybrid Renewable Energy Power Systems: A Review. *Int. J. Precis. Eng. Manuf.-Green Technol.* **2015**, *2*, 99–112. [CrossRef]
23. Li, K.; Song, Y.; Wang, R. Multi-Objective Optimal Sizing of HRES under Multiple Scenarios with Undetermined Probability. *Mathematics* **2022**, *10*, 1508. [CrossRef]
24. Maleki, A.; Khajeh, M.G.; Ameri, M. Optimal sizing of a grid independent hybrid renewable energy system incorporating resource uncertainty, and load uncertainty. *Int. J. Electr. Power Energy Syst.* **2016**, *83*, 514–524. [CrossRef]
25. Bruno, F.; Alexandre, S.; Augusto, B.L. Contracting Strategies for Renewable Generators: A Hybrid Stochastic and Robust Optimization Approach. *IEEE Trans. Power Syst.* **2015**, *30*, 1825–1837.
26. Bornapour, M.; Hooshmand, R.A.; Khodabakhshian, A.; Parastegari, M. Optimal stochastic scheduling of CHP-PEMFC, WT, PV units and hydrogen storage in reconfigurable micro grids considering reliability enhancement. *Energy Convers. Manag.* **2017**, *150*, 725–741. [CrossRef]
27. Reddy, S.S.; Sandeep, V.; Jung, C.M. Review of stochastic optimization methods for smart grid. *Front. Energy* **2017**, *11*, 197–209. [CrossRef]
28. Gabrel, V.; Murat, C.; Thiele, A. Recent advances in robust optimization: An overview. *Eur. J. Oper. Res.* **2014**, *235*, 471–483. [CrossRef]
29. Sun, X.A.; Conejo, A.J. *Robust Optimization in Electric Energy Systems*; Springer: Cham, Switzerland, 2021.
30. Saeedi, M.; Moradi, M.; Hosseini, M.; Emamifar, A.; Ghadimi, N. Robust optimization based optimal chiller loading under cooling demand uncertainty. *Appl. Therm. Eng.* **2019**, *148*, 1081–1091. [CrossRef]
31. Mojtaba Mahmoudi, M.A.; Khodayifar, S. Demand Response Management in Smart Homes Using Robust Optimization. *Electr. Power Compon. Syst.* **2020**, *48*, 817–832. [CrossRef]
32. Shabanzadeh, M.; Sheikh-El-Eslami, M.K.; Haghifam, M.R. The design of a risk-hedging tool for virtual power plants via robust optimization approach. *Appl. Energy* **2015**, *155*, 766–777. [CrossRef]
33. Billionnet, A.; Costa, M.C.; Poirion, P.L. Robust optimal sizing of a hybrid energy stand-alone system. *Eur. J. Oper. Res.* **2016**, *254*, 565–575. [CrossRef]
34. Keyvandarian, A.; Saif, A. Optimal sizing of a reliability-constrained, stand-alone hybrid renewable energy system using robust satisficing. *Renew. Energy* **2023**, *204*, 569–579. [CrossRef]

35. Alqunun, K.; Crossley, P.A. Rated Energy Impact of BESS on Total Operation Cost in a Microgrid. In *2016 IEEE Smart Energy Grid Engineering, Oshawa, ON, Canada, 21–24 August 2016*; Institute of Electrical and Electronics Engineers: Piscataway, NJ, USA, 2016; p. 110.
36. Korovushkin, V.; Boichenko, S.; Artyukhov, A.; Ćwik, K.; Wróblewska, D.; Jankowski, G. Modern Optimization Technologies in Hybrid Renewable Energy Systems: A Systematic Review of Research Gaps and Prospects for Decisions. *Energies* **2025**, *18*, 4727. [CrossRef]
37. Bemporad, A.; Morari, M. Control of systems integrating logic, dynamics, and constraints. *Automatica* **1999**, *35*, 407–427. [CrossRef]
38. Bertsimas, D.; Sim, M. *The Price of Robustness*; Technical Report; INFORMS: Linthicum, MD, USA, 2001.
39. Associazione Nazionale Energia del Vento. *Il Potenziale Eolico Italiano*; Technical Report; ENEA: Rome, Italy, 2017.
40. Monforti, F.; Huld, T.; Bódis, K.; Vitali, L.; D'Isidoro, M.; Lacal-Arántegui, R. Assessing complementarity of wind and solar resources for energy production in Italy. A Monte Carlo approach. *Renew. Energy* **2014**, *63*, 576–586. [CrossRef]
41. Solargis Prospect Website. Available online: https://apps.solargis.com/prospect (accessed on 16 October 2025).
42. Renewable Ninja. Available online: https://www.renewables.ninja/ (accessed on 16 October 2025).
43. Bellinguer, K.; Girard, R.; Bocquet, A.; Chevalier, A. *ELMAS: A One-Year Dataset of Hourly Electrical Load Profiles from 424 French Industrial and Tertiary Sectors Supplementary Material: Data Analysis*; ELMAS: London, UK, 2023.
44. EMBER Website. Available online: https://ember-energy.org/data/european-wholesale-electricity-price-data/ (accessed on 16 October 2025).
45. Sens, L.; Neuling, U.; Kaltschmitt, M. Capital expenditure and levelized cost of electricity of photovoltaic plants and wind turbines – Development by 2050. *Renew. Energy* **2022**, *185*, 525–537. [CrossRef]
46. Wood Mackenzie Website. Available online: https://www.woodmac.com/ (accessed on 16 October 2025).
47. Spiller, M.; Rancilio, G.; Bovera, F.; Gorni, G.; Mandelli, S.; Bresciani, F.; Merlo, M. A Model-Aware Comprehensive Tool for Battery Energy Storage System Sizing. *Energies* **2023**, *16*, 6546. [CrossRef]
48. Moretti, L.; Martelli, E.; Manzolini, G. An efficient robust optimization model for the unit commitment and dispatch of multi-energy systems and microgrids. *Appl. Energy* **2020**, *261*, 113859. [CrossRef]